BioEnergy Research
https://doi.org/10.1007/s12155-023-10595-6

Design of Experiments Study on Scottish Wood Biochars and Process Parameter Influence on Final Biochar Characteristics

Mohammad Umair Jamal[1] · **Ashleigh J. Fletcher**[1]

Received: 27 October 2022 / Accepted: 31 March 2023

Abstract

Native Scottish wood samples were investigated as potential, locally sourced, raw materials for biochar production. Screening experiments identified pure softwood as the preferable feedstock. Influence of operational parameters, i.e. activating gas flow rate (CO_2), heating ramp rate and contact time on final biochar characteristics, was investigated using design of experiments. Surface area and biochar yield were selected as response variables. Minitab was used to define experimental run conditions and suggested an optimal output at 60 min contact time and 15 °C/min ramp rate for maximum responses. The highest surface area (764 m^2/g) was achieved at 850 °C from softwood, albeit with a low yield of 15%. Under optimised conditions, the observed surface area was 613 m^2/g with ~ 18% yield. Pareto charts suggested no influence of gas flow rate on chosen responses, which correlated well with experimental data. Pore structure was a combination of micro- and mesopores with average pore widths of 3–5 nm and an average point of zero charge of 7.40 ± 0.02. Proximate analysis showed an increase in fixed carbon content from 20%, in the feedstock, to 80%, in the optimised biochar. Morphological analysis showed a layered carbon structure in the biochars. The results show the significance of the selected feedstock as a potential source of biochar material and the relevance of interplay of operational variables in biochar development and their final characteristics.

Keywords Pyrolysis · Minitab · DoE · Activated carbon · Wood · Surface area

Introduction

Biochar is the black carbonaceous residue formed from thermochemical conversion of biomass in an inert atmosphere, providing a mechanism to lock in the carbonaceous material rather than releasing greenhouse gas emissions in degradation pathways of the organic matter. These materials require similar or superior performance than commercially used activated carbons for their implementation across different applications, which is achieved by a combination of cheap availability of feedstock, accompanied by diverse physical and chemical properties, giving carbon-rich biochars the potential to be used in a range of applications, including soil amendment, such as enrichment fertilisers [1, 2], catalysts [3], adsorbents [1], and in energy storage [4].

✉ Mohammad Umair Jamal
umair.jamal@strath.ac.uk

Ashleigh J. Fletcher
ashleigh.fletcher@strath.ac.uk

[1] Chemical and Process Engineering, University of Strathclyde, 75 Montrose Street, Glasgow G1 1XL, UK

Recent steps towards creating a circular economy has seen a drive to produce biochars from renewable sources, providing added value to waste streams; however, production is currently unregulated. Notably, biochar production offers scope for ad hoc production, with opportunity to tailor products to target applications. Such bespoke materials, manufactured from regenerative sources, with comparable characteristics to commercially produced activated carbons can potentially help to reduce the overall carbon footprint multiple industrial processes.

Biochars often have well-developed pore networks, ranging from micro- to macropores, and high surface areas that make them suitable for adsorption. The pore network extends throughout the material and provides active binding sites for heavy metals that readily sorb on the surface and within the pore network. Biochars made from renewable sources gave comparable adsorption capacities to commercial activated carbons, even though the surface areas are significantly smaller [5]. As a consequence of these characteristics, biochars produced from different feedstocks, such as walnut wood [6] and rosid angiosperm [7], have been used in water treatment applications. In addition to water

Published online: 15 April 2023

treatment, biochars derived from rice husk have been used in acid catalysis [8], while pyrolysed hard wood biochars have found potential application in biodiesel production [9]; biochars as soil enhancement materials can maintain nutrients within soil and control cation exchange, which reduces nutrient leaching from soils [5], while potassium hydroxide-activated biochar offers potential within supercapacitors [10].

There are several parameters involved in the production of biochars: operating temperature, gas flowrate, residence time, furnace ramp rate, and pressure that can influence the yield and quality of the final product. Pyrolysis temperature is considered one of the key factors influencing the properties of biochars; the breakdown of heavy hydrocarbons decreases the quantity of the final product, as more volatiles are removed from the system [11]. Researchers have reported a reduction in biochar yield on increasing the pyrolysis temperature [12, 13], which is expected, as, at high temperatures, secondary reactions occur that further breakdown the char formed at initial temperatures into liquid and gaseous phases, i.e. releasing more volatile components [14]. While higher temperatures enable the development of micropores and an enhanced pore structure [15], a disadvantage of extreme temperatures is that the formation of ash hinders the growth of the pore network and surface area [16], and a fine balance exists in determining the optimal temperature for biochar formation. By contrast, too low a temperature can result in insignificant changes in pore volume and surface area, as the system is unable to completely devolatilise volatile constituents, and the final product may be subject to pore blockage and an underdeveloped pore network [17]. Previous studies indicate that a temperature range between 400 and 800 °C is most appropriate for biochar production. A low heating rate mitigates the possibility of thermal cracking of biomass and rules out secondary pyrolysis reactions to enhance the biochar yield [14]. A very high heating rate would melt the biochar particles and increase the gaseous and liquid components, thereby decreasing the quantity of the final product [18]. An excessive heating rate also results in accumulation within particles, resulting in blocked pore entrances, due to shortage of time for the volatile matter to diffuse [19], while depolymerisation of biomass and prevalence of secondary pyrolysis result in a reduced biochar yield [20] and can decrease surface area [21]. To avoid micropore coalescence or collapse of the carbon matrix altogether, a high rate of volatile matter generation must be avoided [18], which rules out the use of high heating rates; hence, an optimum range of 10 and 30 °C/min is preferred. Residence time is influenced by temperature, gas flowrate, and heating rate; to promote repolymerisation, and improve biochar yield, sufficient residence time is necessary for reaction [22]; however, several researchers have reported that the yield is not proportional to residence time [23, 24]. Residence times between 30 and 60 min have been reported to yield maximum pore volume for chemically activated biochars from corn cob [25], while an increase in the surface area was reported by for residence time increasing from 10 to 60 min [26]; however, further increase reduced surface area. Complications, arising from interaction between other process conditions and residence time, make it a challenging parameter to analyse; hence, it is a key component to investigate during biochar production with residence times between 20 and 60 min being of interest. By contrast, the influence of pressure on biochar production is relatively straightforward. Extreme, high pressures prevent the release of volatile matter from the system and result in the formation of spherical cavities [27], with continuous decrease in surface areas reported upon increasing the pressure from 1 to > 20 bar [27, 28]. Pressures slightly higher than atmospheric pressure can increase the residence time of reaction constituents, which assists char formation [29], and carbon content in the final product was suggested to be pressure dependent. During pyrolysis, vapours are formed, and these can participate in reactions with the char, modifying its characteristics if not purged from the system [14]. Carrier gases are used to ensure an inert atmosphere for pyrolysis, and nitrogen is the most common carrier gas used being cheaper and more readily available than other inert gases. Increased gas flowrate has been shown to marginally decrease the biochar yield, due to the removal of vapours from the system, preventing repolymerisation [14]; previous work has shown a reduction in yield from 28.4 to ~ 27% on increasing the nitrogen flowrate from 50 to 400 mL/min [30], with similar observations for other systems [5] suggesting that low to moderate flowrates will produce little effect on yield. By contrast, gas flowrate has been shown to markedly affect surface area and total pore volume, with an increase in nitrogen flowrate (50 to 150 mL/min) reported to cause an increase of > 300 m^2/g in surface area and a ten-fold increase in total pore volume for Algerian date pits derived activated carbon [31]. Notably, very high gas flowrates decrease biochar yield and pore volume [31, 32]; hence, moderate gas flowrates between 150 and 300 mL/min are suggested for optimum characteristics.

Previous studies have discussed the relationship between biochar performance and process parameters [33, 34]. However, there is a limitation and lack of understanding of the synergistic effects of these parameters on produced biochars. Feedstock with different physical and chemical compositions react differently to operational parameters and produce biochars with variability in characteristics [35]. Material selection is an important step prior to biochar production. Parent material characteristics can be influenced by climatic conditions [36]. To ensure profitability, the cost incurred in procuring the raw material and transforming it into bespoke materials for chosen applications should offer a reasonable benefit. In this study, the raw material utilised was native Scottish wood, and screening experiments assisted in the

selection between hardwood and softwood, both abundantly available. Locally procured raw material provides a considerable reduction in carbon footprint associated with supply and transport, offering the potential for circularity in the formation of biochar materials for possible applications. This work adopts a design of experiments approach to develop an understanding of the synergistic effects of selected process conditions on biochar characteristics and inform biochar production for such wood sources.

Methodology

The wood samples used in this study were procured from Sustainable Thinking Scotland C.I.C. (Kinneil Estate, Bo'ness, Scotland) and obtained from a walled garden in a 200-acre estate. Wood samples included birch, oak, ash, Scots pine, Sitka spruce, and Western red cedar. Table 1 gives an overview of the sample mix used in the study.

Samples A and B were developed to give a comparison between biochars produced from soft and hardwoods. A design of experiments (DoE) approach was adopted, based on a comprehensive literature review. Screening experiments were performed on samples A and B to identify the type of wood to be used for the DoE study. The results of the preliminary runs on samples A and B were refined, and DoE was applied to sample C. Parameter scoping helped develop DoE runs to investigate a wider parameter space, utilising statistical analysis of variance (ANOVA) using Minitab to determine responses arising due to multiple factors changing simultaneously [37]. This provides a deeper understanding of the systematic factors that have statistical influence on the chosen responses.

Design of Experiments (DoE)

DoE is a multipurpose approach that helps in determining a relationship between input variables against a chosen response. Based on the situation, different design types can be applied to a system. *Comparison* investigates a single factor between different combinations using *t*-, *Z*-, or *F*-tests. *Variable screening* uses factorial designs to analyse the significance of input variables on the overall performance of a system or process. *Transfer function optimisation* allows study of the relationship between relevant input variables to the specified output. *System optimisation* uses the transfer function to improve the overall performance of the system. Finally, *robust design* is aimed at mitigating the effects of system variation without root cause elimination [38].

In this study, a full factorial design (FFD) which falls under variable screening was used to assess possible interactions of input variables as opposed to the traditional one factor at a time approach. The screening runs were based on three variables: contact time with activating agent (CO_2), flowrate of activating gas, and furnace temperature. Two temperatures (600 and 850 °C) were chosen based on a review of the literature, to study the difference in the types of

Table 1 Feedstock for biochar production

Sample	Wood type	Species
A	Predominantly softwood	Ash, birch, oak, Scots pine, Sitka spruce, Western red cedar
B	Predominantly hardwood	Ash, Downey birch, oak, Scots pine, Sitka spruce, Western red cedar
C	100% softwood	Scots pine, Sitka spruce, Western red cedar

Table 2 Process conditions, yields, and textural properties for biochars produced using wood samples A and B (ramp rate = 15 °C/min)

Exp	Sample code	CO_2 flowrate (mL/min)	Temp (°C)	Contact time (min)	Biochar weight (g)	Yield (%)	Surface area (m^2/g)	Micropore volume (cm^3/g)	Total pore volume (cm^3/g)	Average pore width (nm)
S1	250S600-20A	250	600	20	6.53	21.8	544	0.18	0.26	3
S2	250S600-60A	250	600	60	6.20	20.7	538	0.18	0.25	3
S3	250S850-20A	250	850	20	5.30	17.7	597	0.20	0.29	3
S4	100S850-60A	100	850	60	4.41	14.7	764	0.22	0.42	5
S5	250H600-20B	250	600	20	7.59	25.3	525	0.17	0.25	3
S6	250H600-60B	250	600	60	6.96	23.2	544	0.18	0.27	3
S7	250H850-20B	250	850	20	5.16	17.2	573	0.19	0.26	3
S8	100H850-60B	100	60	100	4.54	15.1	714	0.23	0.34	4

produced biochars, as well as yields. Thermal CO_2 activation improves sorption characteristics of biochar and forms new functional groups, creating a more uniform porous structure, and is quicker than chemical activation. Flowrates of 100 or 250 mL/min were used with residence times of 20 and 60 min.

Screening identified softwood as a more desirable feedstock; hence, DoE (using FFD) was applied to pure softwood samples. A mean temperature of 725 °C was used with three variables: contact time (20 and 60 min), gas flowrate (100 and 250 mL/min), and the heating ramp up rate (15 and 30 °C/min) for the full factorial design (FFD). Minitab was used to generate the FFD, which resulted in a total of $2^3 = 8$ experiments for 3 factors with a high and low setting each [39]. The runs were randomised to minimise effects of factors that cannot be controlled. Centre points were omitted from the model to reduce excess material waste and minimise equipment usage and power consumption, but the model was allowed to run interactions up to third order. Biochar yield and surface area were considered as the two design responses as the economic feasibility and performance of the biochars are governed by these properties.

Nomenclature

Sample names were developed as per: The first three digits (e.g. 250 or 100) represent the gas flowrate. 'S' and 'H' denote either softwood or hardwood; the middle set of values (600, 850, 725) represent the pyrolysis temperatures, followed by residence time and sample category, e.g. 20A or 60C. Thus, the sample 250S725-60C represents a gas flowrate of 250 mL/min, for a softwood sample pyrolysed at 725 °C with a residence time of 60 min, from wood batch C. All experiments were conducted at a heating rate of 15 °C/min, with the exception of samples marked '/30', where the ramp rate was increased to 30 °C/min.

Pyrolysis

Prior to combustion, the wood samples were divided into cubes of sides ~ 5 cm. These smaller cubes were washed with de-ionised water to remove dust and oven dried at 100 °C for 24 h. For combustion, a precursor weight of 30 ± 0.1 g was used. The sample was equally distributed into four crucibles fitted with lids, all placed inside the Thermconcept KLS 10/12/WS muffle furnace. A CO_2 flow of 250 mL/min was maintained over the sample for 40 min to ensure an inert atmosphere and the furnace set to the corresponding temperature and dwell time. Following this, the gas flowrate was adjusted to the values detailed in Tables 2 and 3 and heating begun. After each run was complete, the flow of gas was switched off once the furnace reached room temperature, and the sample

Table 3 Process conditions, yields and textural properties for biochars produced wood sample C

Exp	Sample code	CO_2 flowrate (mL/min)	Temp (°C)	Contact time (min)	Biochar weight (g)	Yield (%)	Surface area (m^2/g)	Micropore Volume (cm^3/g)	Total pore volume (cm^3/g)	Average pore width (nm)	Fixed carbon (%)	Volatile matter (%)
	Feedstock										20.3	79.7
	Ramp rate = 15 °C/min											
D1	250S725-60C	250	725	60	5.30	17.7	613	0.19	0.36	3	80.0	20.0
D2	100S725-60C	100	725	60	5.27	17.6	613	0.19	0.35	3	86.0	14.0
D3	250S725-20C	250	725	20	6.08	20.3	558	0.18	0.29	4	80.5	19.5
D4	100S725-20C	100	725	20	6.31	21.0	581	0.19	0.29	5	80.0	20.0
	Ramp rate = 30 °C/min											
D5	250S725-60/30C	250	725	60	4.40	14.7	613	0.19	0.37	5	77.3	22.7
D6	100S725-60/30C	100	725	60	3.65	12.2	553	0.18	0.43	4	73.4	26.6
D7	250S725-20/30C	250	725	20	6.08	20.3	544	0.18	0.27	4	85.1	14.9
D8	100S725-20/30C	100	725	20	6.07	20.2	544	0.17	0.28	4	83.5	16.5

Table 4 Analysis of variance results for yield and surface area

Yield					
Source	DF	Adj SS	Adj MS	*F value*	*p value*
Model	3	5.9828	1.99427	25.88	0.004
Linear	2	5.3330	2.66650	34.61	0.003
Contact time	1	4.3808	4.38080	56.86	0.002
Ramp rate	1	0.9522	0.95220	12.36	0.025
2-way interactions	1	0.6498	0.64980	8.43	0.044
Contact time*ramp rate	1	0.6498	0.64980	8.43	0.044
Error	4	0.3082	0.07705		
Total	7	6.2910			
Surface area					
Model	2	4943	2471.6	5.96	0.048
Linear	2	4943	2471.6	5.96	0.048
Contact time	1	3403	3403.1	8.20	0.035
Ramp rate	1	1540	1540.1	3.71	0.112
Error	5	2075	414.9		
Total	7	7018			

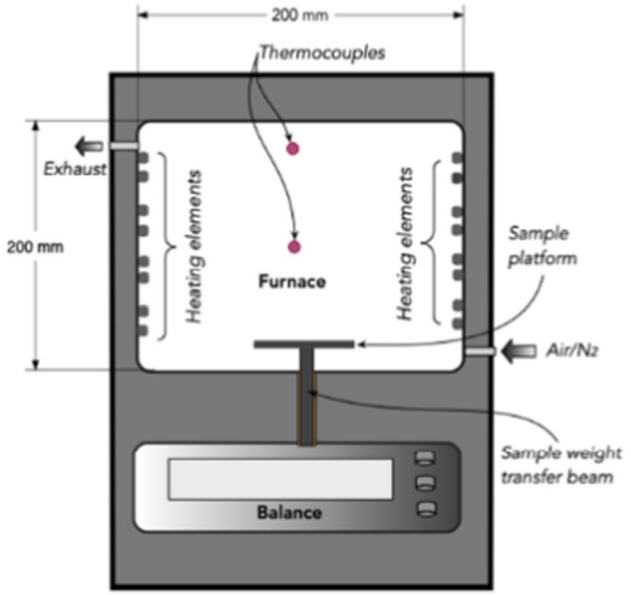

Fig. 1 Schematic diagram of muffle furnace equipped with a weighing system (licence number—5,501,811,254,585) [40]

was allowed to cool overnight. Figure 1 shows a schematic diagram of the muffle furnace used for pyrolysis.

Biochar weight was calculated once the samples had reached room temperature. The yield of the sample is calculated using Eq. 1:

$$Biochar\ yield\ (\%) = \frac{produced\ biochar\ weight\ (g)}{precursor\ weight\ (g)} * 100 \quad (1)$$

Analysis and Characterisation

Porous Structure Characterisation

The biochar sample was crushed to a powdered form prior to analysis, performed using nitrogen adsorption at – 196 °C on a Micrometrics ASAP 2420 system (99.99% nitrogen adsorbate). Degas was performed at 200 °C for 240 min (10 °C/min heating rate). A total of 49 points were taken on the adsorption branch and 30 on the desorption branch. Specific surface area and pore volume distribution of the samples were determined using Brunauer–Emmett–Teller (BET) model [41].

Fourier Transform Infrared Spectroscopy (FTIR)

The biochars were crushed to a powdered form, and a small amount of sample (~ 0.2 g) was placed on the sampling surface. An ABB IR Instrument MB 300 series was used to characterise the functional groups on the surface of the biochar samples using attenuated total reflectance (ATR) for analysis. A total of 32 scans were taken in transmittance mode. The spectra were recorded at 4 cm^{-1} resolution between 500 and 4000 cm^{-1}.

Proximate Analysis

Thermogravimetry was used to carry out proximate analysis of representative biochar samples. The technique employed [42] closely follows the British Standard (BS1016) method. Approximately 5–10 mg of crushed sample was placed in a crucible and analysed using a NETZSCH STA 449 F3 Jupiter system. The crucible was initially tared under a nitrogen gas flow of 50 mL/min, and the mass allowed to stabilise under the same gas flowrate and initial mass recorded. The sample was heated to 120 °C and allowed to stabilise. Subsequently, crucible mass was recorded, and the temperature increased to 920 °C, and held for 3 min, before the mass reading was recorded. Finally, the temperature was reduced to 820 °C, and the flowing gas switched to 50 mL/min of pressurised air. The crucible was allowed to stabilise, and a final mass reading was taken at ambient temperature.

Scanning Electron Microscopy (SEM)

SEM was used to capture the structural characteristics of the biochar surface. A small solid portion was clipped from a biochar cube and placed into the apparatus (Tungsten low-vacuum JEOL JSM-IT100 InTouchScope SEM). Images were captured at 10 µm with × 1000 magnification.

The beam current was kept constant at 35 with a voltage difference of 20 kV.

Point of Zero Charge (PZC)

Salt addition method was used to perform PZC analysis [43]. A 40-mL aliquot of 0.1 M $NaNO_3$ was adjusted to five pH values between 3 and 11. Solutions of 0.1 M NaOH and 0.1 M HCl were used to attain the desired pH. Powdered biochar (~0.2 g) was added to the beakers and agitated at 450 rpm for 24 h. The final solution was filtered and the pH of the permeate was measured. The difference between the initial and final pH values of the samples was calculated, and the change in pH versus initial value was plotted to identify the PZC.

Contact Angle Measurement

Sessile drop method [44] was used to determine the contact angle between the biochar surface and a water drop. Biochar samples were crushed, and a small amount of powder was placed on a microscopic glass slide. The lump was then smoothed by placing another slide on top which was removed before taking measurements. The analysis was performed on a Krüss Scientific Drop Shape Analyser DSA25B. To measure the contact angle, a small droplet of water (~0.5 mL) was dropped onto the sample from a height less than 1 cm, and photographs were taken at intervals of 1, 2, and 3 s using Krüss Advance software.

Results and Discussion

Minitab Outputs

Regression Analysis

Minitab was used to analyse the dataset obtained from the DoE runs. The regression equations for the two responses, yield (Y1) and surface area (Y2), are shown below in Eqs. 2 and 3, respectively. For analysis of the factorial design, a stepwise method was used, which works by combining forward selection and backward elimination procedures. The forward selection approach determines the variables to retain in a model. In forward selection, the added variable is never removed. By contrast, the backward elimination procedure removes terms from the initial model that have the smallest adjusted sum of squares. Determining whether a variable is added or removed from the model is based on the 'Alpha to enter' and 'Alpha to remove' value. If the *p value* of a variable is less than the 'Alpha to enter' value, it is retained in the model and vice versa. In this study, both alpha values were set to 0.15, which is the system default.

$$Yield(Y1) = 6.20 + 0.0058A + 0.0300C - 0.001900AC \quad (2)$$

$$Surface\ area\ (Y2) = 577.8 + 1.031\ Contact\ time\ (min) - 1.85\ Ramp\ rate\left(^{\circ}C/min\right) \quad (3)$$

where A is contact time (min) and C is ramp rate (°C/min). Note that variable B (gas flowrate) was not found to be significant.

The coefficient of determination (R^2) for Eqs. 2 and 3 was equal to 0.95 and 0.70, respectively. The values indicate that the model can explain over 95% and 70% of variability in the responses of yield and surface area, respectively. The model also suggests that there is no notable variation in the obtained responses arising from changes in flow rate of the activating gas. Figure 2 shows the Pareto chart of standardised effects of variables on the responses.

Analysis of Variance (ANOVA)

Statistical analysis of the input variables, i.e. contact time, flow rate, and ramp rate, was performed to identify single or interaction effects on chosen responses. One way of checking the adequacy of the model uses the *p values* and the *F values* from the ANOVA table generated in Minitab. The data generated for yield and surface area is reported in Table 4. For a model to be significant, its *p value* should be less than the significance level (0.05 for a 95% confidence interval in this

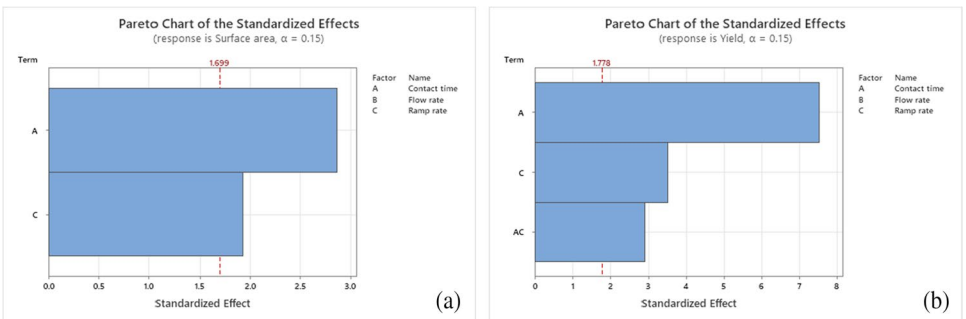

Fig. 2 Pareto chart for variable effects on a surface area and b yield

case), and it should have a high *F value* [45]. In both cases, the *p value* for the model is < 0.05, indicating the models are significant, the model for yield being considerably more accurate compared to the regression for surface area.

It can be seen from the table that contact time and ramp rate have determining effects on yield, with contact time in the furnace being the primary influencing factor with an *F value* of 56.7. There is also a noticeable two-way interaction between contact time and heating ramp rate on yield. The model also suggests no influence of the gas flow rate on biochar yield. For biochar surface area, contact time alone was predicted to be the influencing variable. The ramp rate *p value* was > 0.05 suggesting that this is not a significant variable in surface area determination. No influence of gas flow rate was predicted on surface area.

Response Optimisation

Based on the consideration of the model being statistically significant for both yield and surface area, an optimised response was generated using Minitab with the goal of maximising both of the selected responses. The suggested solution from Minitab included a contact time of 60 min and a ramp rate of 15 °C/min, with no specified value for the gas flow rate, resulting in a surface area of 612 m^2/g and a yield of 5.3 g. The generated solution had a desirability of 78%. The suggested solution was already a part of experiments D1 and D2, both run with a contact time of 60 min and ramp rate of 15 °C/min, with varying flow rates. The observed experimental values for surface area in both cases were 613 m^2/g. In addition, the yield for the two runs was approximately 5.3 g for both runs, which correlates closely to the theoretical predictions. Despite the close relation between theoretical and experimentally obtained data, the low accuracy of the surface area regression presents the need for further analysis of parameter influence on biochar characteristics. The model could be improved by running centre points; however, there is a need to minimise experimental runs to prevent resource utilisation and supplement the idea of sustainability. The following sections further analyse additional characterisation data obtained for the biochars and their relationship with the initial input process variables.

Biochar Yield

Table 2 shows the percentage yield of biochars produced from screening wood samples A and B, under different pyrolysis temperatures, and operating parameters. The trend in yield is as expected, with increasing pyrolysis temperatures resulting in lower quantities of produced biochars [7]. As the temperature is increased, more volatiles are removed from the system, thereby reducing the biomass within the system, hence the final mass of the biochar. It is evident that the final product is determined by a direct combination of the operating parameters. For the softwood chars (Sample A), a low contact time of 20 min and pyrolysis temperature of 600 °C, with a high gas flowrate of 250 mL/min, resulted in the highest biochar yield of 6.5 g. Increasing the contact time to 60 min and keeping the other two parameters constant resulted in a minor reduction in yield of less than 1%. The result suggests that the increment of contact time from 20 to 60 min does not have a significant impact on the product yield. A similar pattern was observed for the hardwood chars (sample B). A maximum yield of 7.6 g was obtained using a high gas flowrate, low pyrolysis temperature, and low contact time. The yield decreased slightly with increased contact time (~ 2%). The lowest yield was obtained at a temperature of 850 °C, with a 60 min residence time and low gas flowrate. Under similar conditions, hardwood samples gave higher yields than the softwood samples. For experiment S1, the softwood yield was 21.8%, and the hardwood biochar was 25.3% under similar parameters (S5). The difference in yield was not considerable for the other runs in both wood batches. This observation, combined with the specific surface areas obtained, indicated that 100% softwood samples were worthy of further investigation.

Table 3 shows the yield of produced biochars from DoE runs. In D1-4, temperature was fixed at 725 °C as an average between the two screening temperatures, and the ramp rate was kept at 15 °C/min. A contact time of 60 min, with both gas flowrates, gave an average yield of ~ 17.5%. This yield was slightly improved when the contact time was reduced to 20 min, giving ~ 20%. The ramp rate was increased to 30 °C/min for D5-8; combined with a high contact time, the yield was further reduced for runs 13 and 14 [18]. The high heating rate however did not seem to affect the yield with shorter residence times. The data suggests that temperature is the primary factor affecting the yield of biochars. There is a noticeable influence of contact time and ramp rate on the yield as previously suggested by the Minitab output, with no discernible influence from gas flow rate.

Porous Structure Characterisation

Figure 3a and b show the adsorption isotherms recorded in the screening study. Experiments S1-4 represent a type II isotherm, governed by adsorption onto microporous solids. The hardwood samples in experiments S5-8 also display an initial high uptake followed by a plateau. There is slight evidence of a final uptake at high relative pressure, which could be attributed to a type II isotherm and multilayer adsorption [46].

Adsorption isotherms obtained for the DoE biochars presented in Fig. 3c and d demonstrate a more prevalent type II/IVa isotherm behaviour with initial high uptakes, followed by a plateau and a slight update at high relative pressure

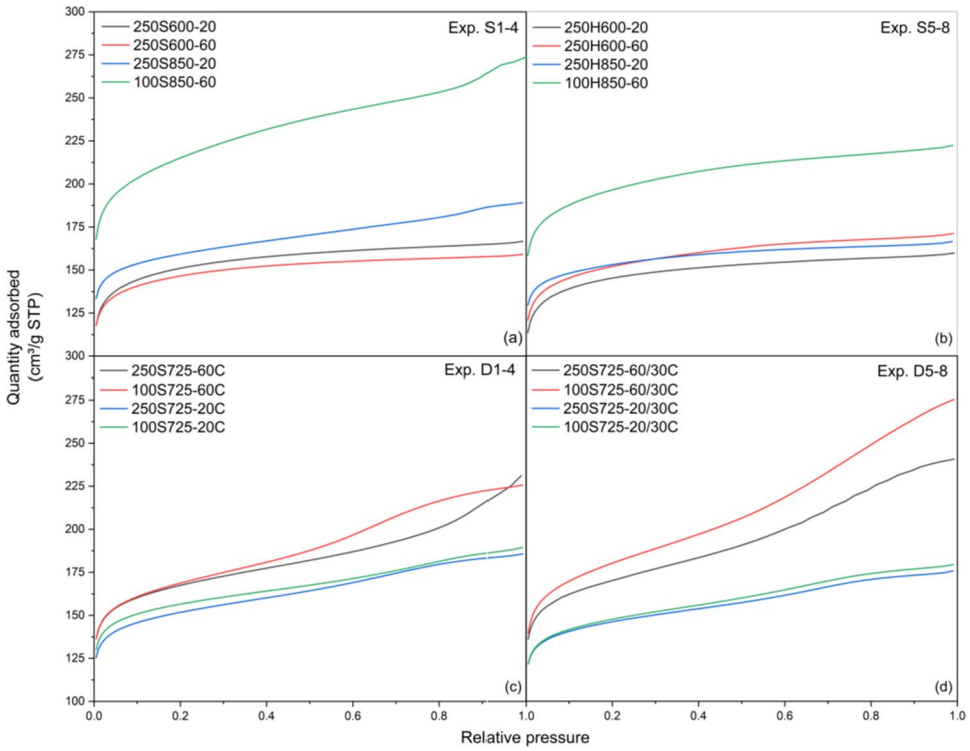

Fig. 3 Adsorption isotherms obtained for biochars

[46]. In general, the evidence of mesoporous nature is more prominent in pure softwood samples (sample C) in the latter experiments.

Table 2 shows the textural data obtained for the screening samples, comprising the surface area, micropore, and total pore volumes, as well as the average pore widths. Similar data on DoE samples is reported in Table 3. The total pore volume of samples is calculated using Eq. 4:

$$Total\ pore\ volume\ (TPV) = (Q_{Sat} * \mathrm{MW}/V_m)/\rho_{liq} \quad (4)$$

where.

Q_{sat} = maximum nitrogen adsorption (in cm^3/g, usually at relative pressure of 0.97 or above).

MW = molecular weight of N_2 (28 g/mol).

V_m = volume occupied by 1 mol of gas (22.4 L).ρ_{liq} = density of liquid N_2 at boiling point (808 g/L)

The *t* plot analysis, developed by Lippens and Boer [47], was used to determine the micropore volumes reported in Tables 2 and 3. It can be inferred that increasing pyrolysis temperatures caused an increase in microporosity. The ratio of micropore volume to TPV is highest in samples with low gas flowrates and higher residence times. At high gas flowrates, $V_{\mathrm{micropore}}/V_{\mathrm{total}}$ ratios are similar for experiments with 20 min hold time at high temperature. The evidence suggests an inverse relationship between microporosity development and residence time. Microporosity is suitable for interactions between small adsorbate species and adsorbents [7], so this can be a useful quantity to optimise. DoE experiments D5 and D6 indicate that a higher ramp rate combined with a longer hold time can enhance mesoporous nature in the biochars, which have previously been shown to be useful for aqueous phase applications [48].

Surface areas were calculated using BET analysis; however, such analysis is highly sensitive to the selected relative pressure range [49], particularly for microporous materials, and the optimal relative pressure range can be determined using the four consistency criteria suggested by Rouquerol et al. [50]: (1) only the range where the product of the adsorbate loading rate and 1 minus the relative pressure is increasing monotonically with the relative pressure should be chosen; (2) the value of BET 'C constant' must be positive. C constant quantifies the adsorbent and adsorbate interactions and is related to the energetics of adsorption in the first adsorbed layer [49]; (3) the selected linear region should encompass monolayer loading corresponding to the relative pressure; and (4) the relative pressure calculated in criterion 3 should be equal to the one calculated from BET theory consonant with monolayer loading with a 20% tolerance. Given the presence of significant microporosity reported in Tables 2 and 3, the Rouquerol correction was applied for all samples produced in this study. The maximum BET surface area was recorded for a pyrolysis temperature of 850 °C with a gas flowrate of 100 mL/min and 60 min residence time with softwood precursor (S4). Shorter residence times produced biochars with lower

surface areas compared to those obtained under similar conditions but with longer hold time. Similar observations of improved surface areas with residence time were reported previously [26]. On average, pyrolysis runs performed at 725 °C produced biochars with higher surface areas. The intermediate temperatures also offered a reasonable trade-off between biochar yield and average pore widths. For DoE runs, lower ramp rates with high residence time can be inferred to be directly proportional to surface area. A reduction in $V_{micropore}/V_{total}$ ratio of these samples also suggests a more openly porous structure [7]. The highest biochar surface areas obtained for 100% softwood chars were higher than other wood-based biochars reported in the literature [7, 51]. As in the case of yield, observations made for surface area supplement the Minitab output with the exception of Experiment D6 where a high ramp rate has resulted in a reduced biochar surface area. This output could possibly be attributed to the reduced accuracy of the model.

Pore width data obtained from Barrett-Joyner-Halenda (BJH) analysis [52] (Tables 2 and 3) further confirms the predominantly microporous nature of the biochars. The average pore widths were largest for runs performed at 725 °C with high ramp rates. As stated above, shorter hold times resulted in increased microporosity, as well as narrower pore widths. Predominantly softwood biochars (S1-4) were almost as microporous as hardwood biochars (S5-8), and sample C (entirely softwood, D1-8) demonstrated the highest mesoporosity. The results indicate a possible application for sample A in the adsorption of small adsorptive species, mainly in gas phase [49], including in carbon capture [51].

Fourier Transform Infrared Spectroscopy

Figure 4a presents the FTIR spectrum obtained for softwood feedstock. In the fingerprint region, between 600 and 1500 cm^{-1}, there is evidence of $CH=CH_2$ vinyl terminals [53]. There is also evidence of loss of the peak from C–OH vibrations in the feedstock at 1000 cm^{-1} from pyrolysis treatment [7]. The heat treatment plays a crucial role in condensation of the carbonaceous skeleton and removes the hydroxyl groups from cellulosic compounds present in the precursors [54].

Figure 4b and c show the FTIR spectra for DoE biochar samples obtained using low and high ramp rates. The observed spectra look identical and not influenced by the change in ramp rates of the experimental runs. The peaks observed between regions 3800 and 3500 cm^{-1} indicate the presence of hydrogen bonds. This information is further supplemented by peaks between 1600 and 1300 cm^{-1}, as is the case with analysed biochar samples [53]. There are sharp peaks from the biochars between 3000 and 2600 cm^{-1} that could be due to C-H stretching bonds [7]. There is also strong evidence of C=C bonds with symmetric and asymmetric vibrations and possible conjugation, as well as stretching vibrations with other structures such as oxygen and hydrogen (C=O, C-H) from the spectra in the

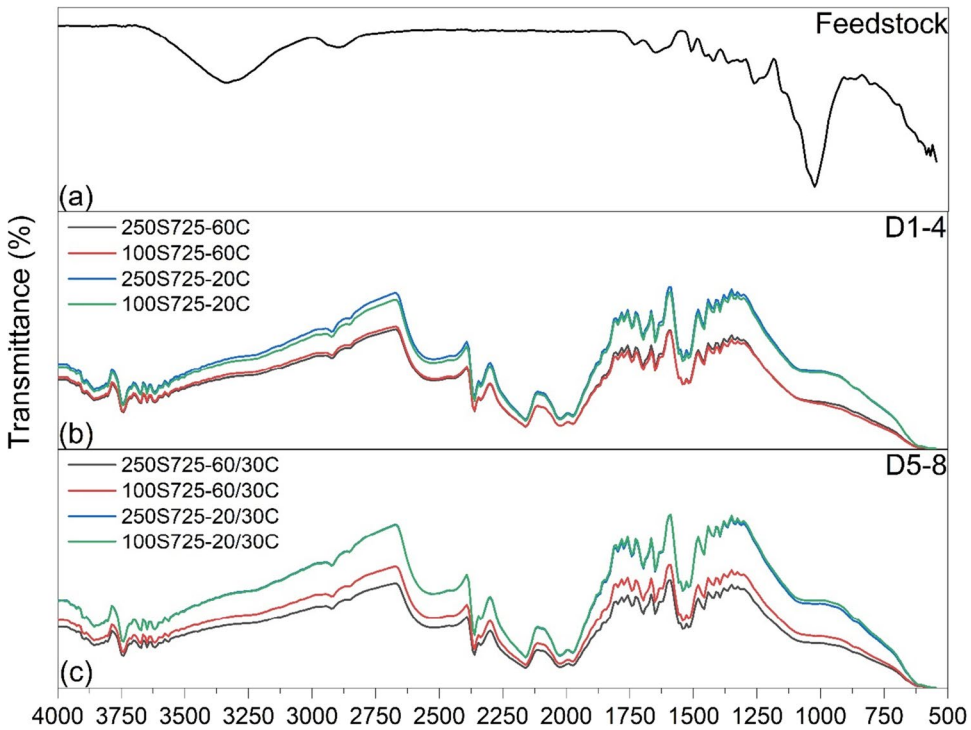

Fig. 4 FTIR spectrum of feedstock and DoE biochars

1600–1800 cm^{-1} region [53]. These functional groups could be the result of the presence of ketones, aldehydes, and carboxylic acids [55]. The results indicate the development of a layered, almost graphene-like carbon arrangement in the aromatic and aliphatic structures of the biochars [2]. There is no quantifiable influence of gas flowrate and residence time on the functional groups present in the samples. It can therefore be noted that temperature continues to be the primary influence on surface chemistry of produced biochars.

Proximate Analysis

The dry ash compositions of the feedstock and DoE biochars obtained from thermogravimetric analysis are reported in Table 3. The samples were treated on a dry basis to remove variability from moisture content and on an ash-free basis due to variability in inorganic forms from the natural precursor. A high contact time in experiments D1 and D2 resulted in a fixed carbon percentage of 80% and a volatile matter content of 20%. This was a significant increase from the fixed carbon content of 20.3% in the feedstock. For experiment D2, under a much lower gas flowrate, the carbon content was increased to 86% and volatiles reduced to 14%. The higher gas flowrate appears to have potentially decreased the temperature of the sample and affected the release of volatile matter as suggested previously [16]. For experiments D3 and D4, with shorter residence time, gas flowrates did not have a considerable impact on fixed carbon and volatile fractions. High heating rates combined with longer residence times result in accumulation of volatile matter [19]. The results obtained in D5 and D6 support this statement, with carbon percentages below 80 and higher volatile content, as opposed to their lower ramp rate counterparts. With a shorter hold period (D7 and D8), the percentages of volatiles reduced significantly, and a positive effect on fixed carbon content was also noted. Residence time was observed to be the key driver for fixed carbon and volatiles, with the fluctuations arising from variable gas flowrates being almost negligible. The results indicate that a higher ramp rate combined with a short residence time has the potential to produce biochars with high fixed carbon content and the lowest fraction of volatiles, albeit with a significant loss in yield.

Scanning Electron Microscopy

Figure 5a–d show the SEM images recorded for lower ramp rate biochars, and Fig. 5e–g display the observations for higher ramp rate biochars. There is evidence of a well-developed pore network in biochars produced at low and high ramp rates. The images at 10 µm and 1000 × magnification suggest that the high pyrolysis temperatures exposed the carbonaceous skeleton of the parent material encompassing an intricate network of pores [56]. A pyrolysis temperature that is sufficiently high is necessary for the removal of the outer biochar layer. The open structure of pores could be attributed to a lower ash content, which reduces the potential for clogging. There is no apparent evidence of influence from different ramp rates on the pore networks developed in the biochars.

Point of Zero Charge

The surface charge of chars produced under different operating conditions appears to be dependent on material origin and surface functional groups, as opposed to chosen DoE variables. The average PZC of the samples in this study was 7.40 ± 0.02. Pyrolysis temperatures influence the pH of wood-based biochars. High temperatures result in the loss of not only volatile matter but also acidic functional groups, i.e. phenols and carboxylic, thereby resulting in more alkaline surface charges [57]. For example, slow pyrolysis treatment of wood-based pellets at 200 °C produced biochars with pH 4.6. Upon increasing the temperature to 600 °C, the resulting biochar had a pH of 9.5 [58]. A similar observation on wood chip biochars pyrolysed at 500 °C was made with biochars having a pH(H_2O) of 8.58 ± 0.01 [59]. Having a neutral/slightly alkaline surface charge indicates potential application in drinking water systems that operate under acidic conditions without much alternation to target anionic species from effluents [57].

Contact Angle Measurement

Biochar wettability is a parameter that can be evaluated through contact angle (CA) measurement [60]. Figure 6a shows water droplet on a clear glass slide, and Fig. 6b shows a similar water droplet on a biochar film. Both images were taken 2 s after water contact. The measurement was repeated for all biochar samples and yielded similar observations. The absorption of water by prepared biochars was seemingly immediate, indicating hydrophilicity and high wettability [60]. Low CA (typically $< 90°$) are achieved in cases where water shows greater affinity to the solid surface [61]. The mechanism for this interaction could potentially be the formation of surface hydrogen bonds and the domination of adhesion forces over repulsive ones. This stabilisation of forces allows water to penetrate porous materials and wet larger surface areas [60]. This observed wettability in case of native Scottish biochars suggests a feasible application in drinking water treatment systems, allowing larger available surface areas for interaction between dissolved target species in water.

Discussion

Examination of the wide range of results obtained for the chars produced within this study suggests significant correlation of biochar properties with parameters used within their

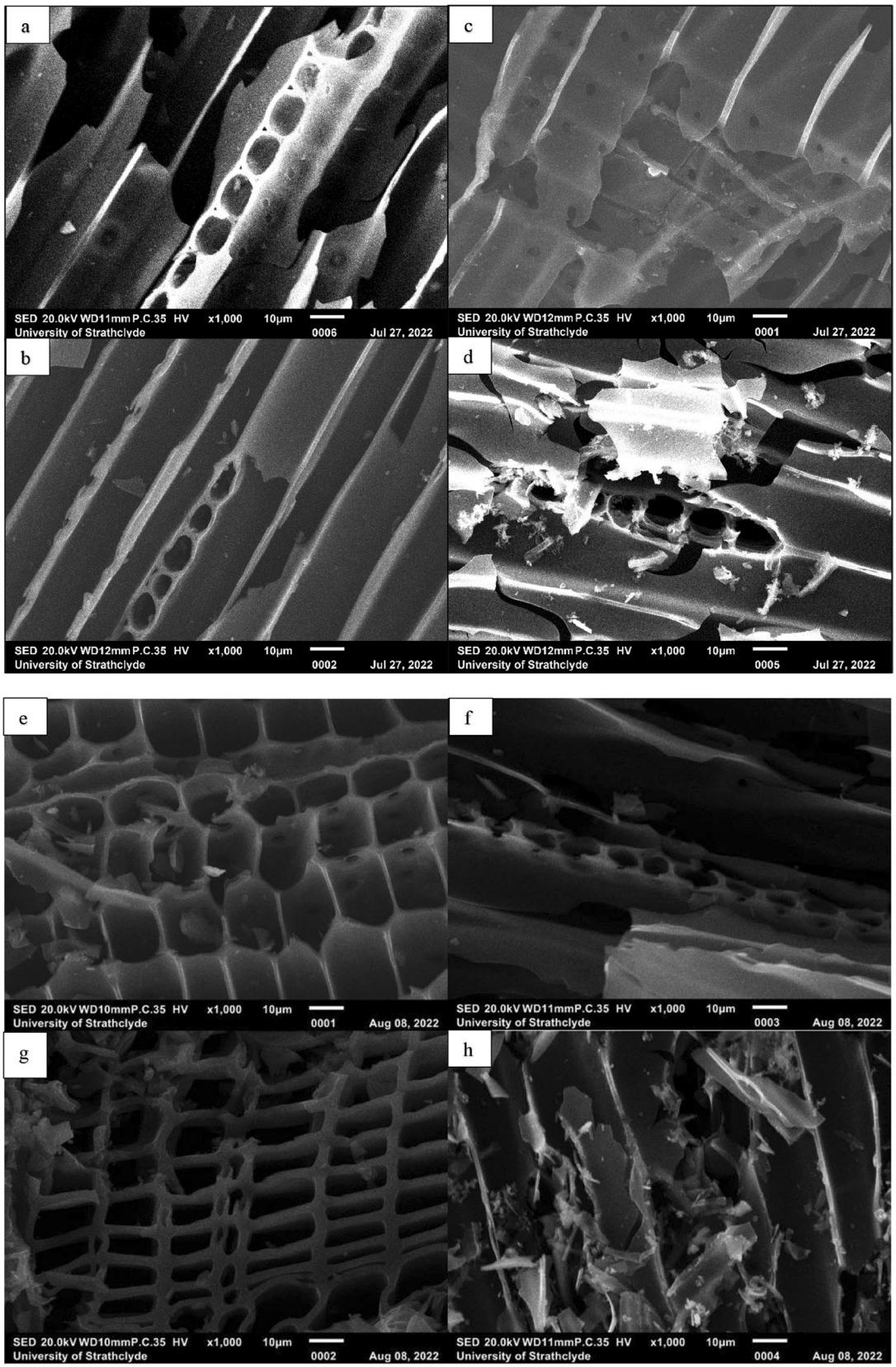

Fig. 5 a–d SEM of biochars with lower ramp rates; e–h SEM of biochars with higher ramp rates.

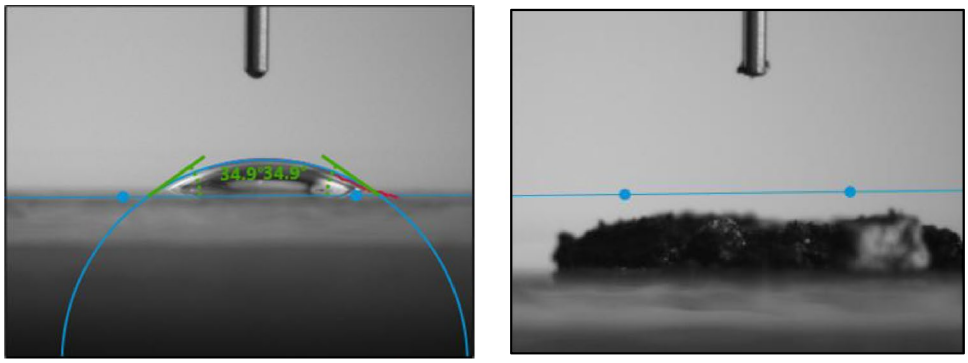

(a) Water droplet on a clear glass slide

(b) Water droplet on biochar surface

Fig. 6 a Water droplet on a clear glass slide. b Water droplet on biochar surface.

production. The surface areas of biochars reported in this study are higher than selected biochars reported in literature [57, 59]. The amount of fixed carbon in wood-based chars appears to be consistent, at around 80%, which was also observed for the DoE biochars. Temperatures above 400 °C were reported to produce a recalcitrant structure resulting from the loss of volatile matter, as well as alkyl and carboxylic groups [62]. The statement further supplements the chemical moiety information obtained from FTIR, suggesting a layered carbon structure. The concentric arrangement of pores in the carbonaceous skeleton is also visible in the SEM images.

Higher temperatures have also been reported to increase alkalinity of biochars [57]. DoE biochars in this work were determined to have an average PZC of 7.40 ± 0.02. In addition to a neutral pH, contact angle analysis of the biochars suggested hydrophilic character. Rattanakam et al. investigated the difference in hydrophilicity of oxidised and un-oxidised wood-based biochars [63], reporting an increase in the hydrophilic behaviour of oxidised biochars. Fir wood-derived biochars for perchlorate adsorption were contrastingly reported to provide a hydrophobic environment, as opposed to the hydrophilic biochars produced in this work [64]. The high surface areas, carbon content, and hydrophilic nature of the biochars produced in this work give them great potential for possible application in water and wastewater treatment systems [57]. Process parameter influence on biochar characteristics appears to be significant, as evidenced by the DoE study and could potentially provide a pathway to produce sustainable biochars catered to specific applications.

Conclusions

Biochars produced from native Scottish woods showed significant influence of pyrolysis operating parameters on the characteristics of the final products. The optimal solution for a design of experiments study on softwood closely resembled data obtained from experimental runs. Gas flow rates were noted as insignificant with contact time having the greatest impact on biochar characteristics. A high residence time not only produced an increase in observed surface area but also appeared to enhance mesoporosity within the pore structure. Spectroscopic analysis indicated the presence of a layered carbon structure in the biochars. The intricate pore network and graphene-like layered porous arrangement are also evident from morphological analysis. All biochars carry an almost neutral surface charge with a hydrophilic nature, indicating potential for application in water treatment systems. The results demonstrate the potential for native Scottish wood samples as a biochar material, with a requirement to consider the influence of manufacturing operating parameters on final biochar characteristics.

Supplementary Information The online version contains supplementary material available at https://doi.org/10.1007/s12155-023-10595-6.

Declarations

Conflict of Interest The authors declare no competing interests.

References

1. Manyà JJ (2012) Pyrolysis for biochar purposes: a review to establish current knowledge gaps and research needs. Environ Sci Technol 46:7939–7954. https://doi.org/10.1021/es301029g
2. Ahmad M, Rajapaksha AU, Lim JE et al (2014) Biochar as a sorbent for contaminant management in soil and water: A review. Chemosphere 99:19–33. https://doi.org/10.1016/j.chemosphere.2013.10.071
3. Lee J, Kim K-H, Kwon EE (2017) Biochar as a Catalyst. Renewable and Sustainable Energy Reviews 77:70–79. https://doi.org/10.1016/j.rser.2017.04.002
4. Liu W-J, Jiang H, Yu H-Q (2019) Emerging applications of biochar-based materials for energy storage and conversion. Energy Environ Sci 12:1751–1779. https://doi.org/10.1039/c9ee00206e
5. Ahmad J, Patuzzi F, Rashid TDU et al (2020) Exploring untapped effect of process conditions on biochar characteristics and applications. Environ Technol Innov 21:101310. https://doi.org/10.1016/j.eti.2020.101310
6. Ghaedi M, Mazaheri H, Khodadoust S et al (2015) Application of central composite design for simultaneous removal of methylene blue and Pb2+ ions by walnut wood activated carbon. Spectrochim Acta A Mol Biomol Spectrosc 135:479–490. https://doi.org/10.1016/j.saa.2014.06.138
7. Idowu GA, Fletcher AJ (2020) The manufacture and characterisation of rosid angiosperm-derived biochars applied to water treatment. Bioenergy Res 13:387–396. https://doi.org/10.1007/s12155-019-10074-x
8. Li M, Chen D, Zhu X (2013) Preparation of solid acid catalyst from rice husk char and its catalytic performance in esterification. Chinese Journal of Catalysis 34:1674–1682. https://doi.org/10.1016/S1872-2067(12)60634-2
9. Dehkhoda AM, West AH, Ellis N (2010) Biochar based solid acid catalyst for biodiesel production. Appl Catal A Gen 382:197–204. https://doi.org/10.1016/j.apcata.2010.04.051
10. Dehkhoda AM, Ellis N, Gyenge E (2014) Electrosorption on activated biochar: effect of thermo-chemical activation treatment on the electric double layer capacitance. J Appl Electrochem 44:141–157. https://doi.org/10.1007/s10800-013-0616-4
11 Roncancio R, Gore JP (2021) CO2 char gasification: a systematic review from 2014 to 2020. Energy Conversion and Management: X 10:100060. https://doi.org/10.1016/j.ecmx.2020.100060
12 Kyzas GZ, Deliyanni EA, Matis KA (2016) Activated carbons produced by pyrolysis of waste potato peels: cobalt ions removal by adsorption. Colloids Surf A Physicochem Eng Asp 490:74–83. https://doi.org/10.1016/j.colsurfa.2015.11.038
13. Marañón E, Sastre H (1991) Heavy metal removal in packed beds using apple wastes. Bioresour Technol 38:39–43. https://doi.org/10.1016/0960-8524(91)90219-A
14. Tripathi M, Sahu JN, Ganesan P (2016) Effect of process parameters on production of biochar from biomass waste through pyrolysis: a review. Renew Sustain Energy Rev 55:467–481. https://doi.org/10.1016/j.rser.2015.10.122
15. Lehmann J, Joseph S (2015) Biochar for environmental management, 2nd edn. Routledge, London
16 Luo L, Xu C, Chen Z, Zhang S (2015) Properties of biomass-derived biochars: combined effects of operating conditions and biomass types. Bioresour Technol 192:83–89. https://doi.org/10.1016/j.biortech.2015.05.054
17. Pallarés J, González-Cencerrado A, Arauzo I (2018) Production and characterization of activated carbon from barley straw by physical activation with carbon dioxide and steam. Biomass Bioenergy 115:64–73. https://doi.org/10.1016/j.biombioe.2018.04.015
18 Leng L, Xiong Q, Yang L et al (2021) An overview on engineering the surface area and porosity of biochar. Science of The Total Environment 763:144204. https://doi.org/10.1016/j.scitotenv.2020.144204
19. Angın D (2013) Effect of pyrolysis temperature and heating rate on biochar obtained from pyrolysis of safflower seed press cake. Bioresour Technol 128:593–597. https://doi.org/10.1016/j.biortech.2012.10.150
20 Ateş F, Pütün E, Pütün AE (2004) Fast pyrolysis of sesame stalk: yields and structural analysis of bio-oil. J Anal Appl Pyrolysis 71:779–790. https://doi.org/10.1016/j.jaap.2003.11.001
21 Chen D, Li Y, Cen K et al (2016) Pyrolysis polygeneration of poplar wood: effect of heating rate and pyrolysis temperature. Bioresour Technol 218:780–788. https://doi.org/10.1016/j.biortech.2016.07.049
22. Park HJ, Park Y-K, Kim JS (2008) Influence of reaction conditions and the char separation system on the production of bio-oil from radiata pine sawdust by fast pyrolysis. Fuel Processing Technology 89:797–802. https://doi.org/10.1016/j.fuproc.2008.01.003
23 Mohamed AR, Hamzah Z, Daud MZM, Zakaria Z (2013) The effects of holding time and the sweeping nitrogen gas flowrates on the pyrolysis of EFB using a fixed–bed reactor. Procedia Eng 53:185–191. https://doi.org/10.1016/j.proeng.2013.02.024
24 Tsai WT, Lee MK, Chang YM (2007) Fast pyrolysis of rice husk: product yields and compositions. Bioresour Technol 98:22–28. https://doi.org/10.1016/j.biortech.2005.12.005
25. Tsai WT, Chang CY, Lee SL (1997) Preparation and characterization of activated carbons from corn cob. Carbon N Y 35:1198–1200. https://doi.org/10.1016/S0008-6223(97)84654-4
26. Zhao B, O'Connor D, Zhang J et al (2018) Effect of pyrolysis temperature, heating rate, and residence time on rapeseed stem derived biochar. J Clean Prod 174:977–987. https://doi.org/10.1016/j.jclepro.2017.11.013
27. Cetin E, Gupta R, Moghtaderi B (2005) Effect of pyrolysis pressure and heating rate on radiata pine char structure and apparent gasification reactivity. Fuel 84:1328–1334. https://doi.org/10.1016/j.fuel.2004.07.016
28 Melligan F, Auccaise R, Novotny EH et al (2011) Pressurised pyrolysis of Miscanthus using a fixed bed reactor. Bioresour Technol 102:3466–3470. https://doi.org/10.1016/j.biortech.2010.10.129
29. Manyà JJ, Roca FX, Perales JF (2013) TGA study examining the effect of pressure and peak temperature on biochar yield during pyrolysis of two-phase olive mill waste. J Anal Appl Pyrolysis 103:86–95. https://doi.org/10.1016/j.jaap.2012.10.006
30 Ertaş M, Hakkı Alma M (2010) Pyrolysis of laurel (Laurus nobilis L.) extraction residues in a fixed-bed reactor: characterization of bio-oil and bio-char. J Anal Appl Pyrolysis 88:22–29. https://doi.org/10.1016/j.jaap.2010.02.006
31. Bouchelta C, Medjram MS, Zoubida M et al (2012) Effects of pyrolysis conditions on the porous structure development of date pits activated carbon. J Anal Appl Pyrolysis 94:215–222. https://doi.org/10.1016/j.jaap.2011.12.014
32. Lua AC, Lau FY, Guo J (2006) Influence of pyrolysis conditions on pore development of oil-palm-shell activated carbons. J Anal Appl Pyrolysis 76:96–102. https://doi.org/10.1016/j.jaap.2005.08.001
33 Hassan M, Liu Y, Naidu R et al (2020) Influences of feedstock sources and pyrolysis temperature on the properties of biochar and functionality as adsorbents: a meta-analysis. Science of The Total Environment 744:140714. https://doi.org/10.1016/j.scitotenv.2020.140714
34 Leng L, Huang H (2018) An overview of the effect of pyrolysis process parameters on biochar stability. Bioresour Technol 270:627–642. https://doi.org/10.1016/j.biortech.2018.09.030
35. Rehrah D, Bansode RR, Hassan O, Ahmedna M (2018) Short-term greenhouse emission lowering effect of biochars from solid organic municipal wastes. Int J Environ Sci Technol 15:1093–1102. https://doi.org/10.1007/s13762-017-1470-4

36. Seow YX, Tan YH, Mubarak NM et al (2022) A review on biochar production from different biomass wastes by recent carbonization technologies and its sustainable applications. J Environ Chem Eng 10:107017. https://doi.org/10.1016/j.jece.2021.107017
37. Deloach R Analysis of variance in the modern design of experiments. American Institute of Aeronautics and Astronautics
38. Durakovic B (2017) Design of experiments application, concepts, examples: state of the art. Periodicals of Engineering and Natural Sciences (PEN) 5 https://doi.org/10.21533/pen.v5i3.145
39. Barad M (2014) Design of experiments (DOE)—a valuable multipurpose methodology. Appl Math (Irvine) 05:2120–2129. https://doi.org/10.4236/am.2014.514206
40. Cao W, Li J, Lin L, Zhang X (2021) Release of potassium in association with structural evolution during biomass combustion. Fuel 287:119524. https://doi.org/10.1016/j.fuel.2020.119524
41. Brunauer S, Emmett PH, Teller E (1938) Adsorption of gases in multimolecular layers. J Am Chem Soc 60:309–319. https://doi.org/10.1021/ja01269a023
42. Warne SSJ (1991) Proximate analysis of coal, oil shale, low quality fossil fuels and related materials by thermogravimetry. TrAC Trends in Analytical Chemistry 10:195–199. https://doi.org/10.1016/0165-9936(91)85021-I
43. Bakatula EN, Richard D, Neculita CM, Zagury GJ (2018) Determination of point of zero charge of natural organic materials. Environ Sci Pollut Res 25:7823–7833. https://doi.org/10.1007/s11356-017-1115-7
44. Usevičiūtė L, Baltrėnaitė E (2020) Methods for determining lignocellulosic biochar wettability. Waste Biomass Valorization 11:4457–4468. https://doi.org/10.1007/s12649-019-00713-x
45. El-Masry EH, Ibrahim HA, Abdel Moamen OA, Zaher WF (2022) Sorption of some rare earth elements from aqueous solutions using copolymer/activated carbon composite: multivariate optimization approach. Advanced Powder Technology 33:103467. https://doi.org/10.1016/j.apt.2022.103467
46. Thommes M, Kaneko K, Neimark AV et al (2015) Physisorption of gases, with special reference to the evaluation of surface area and pore size distribution (IUPAC Technical Report). Pure Appl Chem 87:1051–1069. https://doi.org/10.1515/pac-2014-1117
47 Lippens BC, de Boer JH (1965) Studies on pore systems in catalysts: V. The t method. J Catal 4:319–323. https://doi.org/10.1016/0021-9517(65)90307-6
48. Parsa M, Nourani M, Baghdadi M et al (2019) Biochars derived from marine macroalgae as a mesoporous by-product of hydrothermal liquefaction process: characterization and application in wastewater treatment. Journal of Water Process Engineering 32:100942. https://doi.org/10.1016/j.jwpe.2019.100942
49. Gómez-Gualdrón DA, Moghadam PZ, Hupp JT et al (2016) Application of consistency criteria to calculate BET areas of micro- and mesoporous metal–organic frameworks. J Am Chem Soc 138:215–224. https://doi.org/10.1021/jacs.5b10266
50. Sing KSW (2014) 7 - Assessment of surface area by gas adsorption. In: Rouquerol F, Rouquerol J, Sing KSW et al (eds) Adsorption by Powders and Porous Solids, 2nd edn. Academic Press, Oxford, pp 237–268
51. Kloss S, Zehetner F, Dellantonio A et al (2012) Characterization of slow pyrolysis biochars: effects of feedstocks and pyrolysis temperature on biochar properties. J Environ Qual 41:990–1000. https://doi.org/10.2134/jeq2011.0070
52. Barrett EP, Joyner LG, Halenda PP (1951) The determination of pore volume and area distributions in porous substances. I. Computations from Nitrogen Isotherms. J Am Chem Soc 73:373–380. https://doi.org/10.1021/ja01145a126
53 Nandiyanto ABD, Oktiani R, Ragadhita R (2019) How to read and interpret FTIR spectroscope of organic material. Indonesian Journal of Science and Technology 4:97. https://doi.org/10.17509/ijost.v4i1.15806
54. Lee JW, Kidder M, Evans BR et al (2010) Characterization of biochars produced from cornstovers for soil amendment. Environ Sci Technol 44:7970–7974. https://doi.org/10.1021/es101337x
55. Rey-Mafull CA, Tacoronte JE, Garcia R et al (2014) Comparative study of the adsorption of acetaminophen on activated carbons in simulated gastric fluid. Springerplus 3:48. https://doi.org/10.1186/2193-1801-3-48
56. Chaves Fernandes BC, Ferreira Mendes K, Dias Júnior AF et al (2020) Impact of pyrolysis temperature on the properties of eucalyptus wood-derived biochar. Materials 13:5841. https://doi.org/10.3390/ma13245841
57. Shaheen SM, Niazi NK, Noha E et al (2019) Wood-based biochar for the removal of potentially toxic elements in water and wastewater: a critical review. Int Mater Rev 64:216–247. https://doi.org/10.1080/09506608.2018.1473096
58. Zhang H, Voroney RP, Price GW (2015) Effects of temperature and processing conditions on biochar chemical properties and their influence on soil C and N transformations. Soil Biol Biochem 83:19–28. https://doi.org/10.1016/j.soilbio.2015.01.006
59. Pipíška M, Krajčíková EK, Hvostik M, et al (2022) Biochar from wood chips and corn cobs for adsorption of thioflavin t and erythrosine B. Materials 15
60. Bubici S, Korb J-P, Kučerik J, Conte P (2016) Evaluation of the surface affinity of water in three biochars using fast field cycling NMR relaxometry. Magn Reson Chem 54:365–370. https://doi.org/10.1002/mrc.4391
61. Yuan Y, Lee TR (2013) Contact angle and wetting properties. Springer, Berlin Heidelberg, pp 3–34
62. Jindo K, Mizumoto H, Sawada Y et al (2014) Physical and chemical characterization of biochars derived from different agricultural residues. Biogeosciences 11:6613–6621. https://doi.org/10.5194/bg-11-6613-2014
63. Rattanakam R, Pituya P, Suwan M, Supothina S (2017) Assessment of hydrophilic biochar effect on sandy soil water retention. Key Eng Mater 751:790–795. https://doi.org/10.4028/www.scientific.net/KEM.751.790
64. Fang Q, Chen B, Lin Y, Guan Y (2014) Aromatic and hydrophobic surfaces of wood-derived biochar enhance perchlorate adsorption via hydrogen bonding to oxygen-containing organic groups. Environ Sci Technol 48:279–288. https://doi.org/10.1021/es403711y